Вестник Астраханского государственного технического университета.
Серия: Управление, вычислительная техника и информатика. 2026. № 3
Vestnik of Astrakhan State Technical University.
Series: Management, computer science and informatics. 2026. N. 3
ISSN 2072-9502 (Print), ISSN 2224-9761 (Online)

УПРАВЛЕНИЕ, МОДЕЛИРОВАНИЕ, АВТОМАТИЗАЦИЯ

CONTROL, MODELING, AUTOMATION

Original article
UDK 004.415.2
https://doi.org/10.24143/2072-9502-2026-3-7-18
EDN DCSNLA

Simulation of gas flows in a cyclone dust collector: dynamics of small-scale perturbations in the near-wall region

Egor S. Savin, Alexander V. Khoperskov✉

Volgograd State University,
Volgograd, Russia, khoperskov@volsu.ru✉

Abstract. The separation of solid particles from the gas stream in cyclone devices is governed by complex turbulent flows within the working chamber. Therefore, the fidelity of gas dynamics modeling is a key factor in predicting the separation efficiency of the inlet flow. In this study, we employ Large Eddy Simulation (LES) within the ANSYS Fluent framework. We compare these results with the Reynolds Stress Model (RSM), which is the most accurate and widely used anisotropic turbulence model for RANS-based cyclone simulations. To perform a refined analysis of the temporal structure of perturbations in the near-wall region, we propose using velocity increments or calculating local fluid acceleration. This approach enables the identification of the fine-scale dynamics of rapid perturbations that are typically obscured by conventional time-averaging methods. Computational experiments using the LES model reveal the presence of fine-scale elongated structures known as near-wall streaks. These structures move along the solid surfaces in the near-wall region of the cyclone. Such streaky structures are generated within the boundary layer. The proposed method based on local acceleration allows for a detailed investigation of subgrid-scale processes in the LES framework. The local accelerations associated with these streaky perturbations can reach magnitudes of 100 g. This may negatively impact separation efficiency and intensify abrasive wear on the walls. We provide estimates for the phase velocity and lifetime of these near-wall nonlinear perturbations. These estimates are consistent with Direct Numerical Simulation (DNS) results for vortex structure generation in boundary layers. Conversely, the RSM turbulence model fails to resolve these streaky structures through the analysis of local acceleration fields.

Keywords: cyclone separator, turbulent gas flow, computational fluid dynamics, large eddy simulation

Acknowledgments: this work was supported by the Ministry of Science and Higher Education of the Russian Federation within the framework of the project FZUU-2026-0005. The computational resources of the Volgograd State University Supercomputing Center and the Laboratory of Artificial Intelligence and Data Analysis were utilized.

For citation: Savin E. S., Khoperskov A. V. Simulation of gas flows in a cyclone dust collector: dynamics of small-scale perturbations in the near-wall region. *Vestnik of Astrakhan State Technical University. Series: Management, computer science and informatics*. 2026;3:7-18. (In Russ.). https://doi.org/10.24143/2072-9502-2026-3-7-18. EDN DCSNLA.

Научная статья

Моделирование потоков газов в циклонном пылеуловителе: динамика мелкомасштабных возмущений в пристеночной зоне

Егор Сергеевич Савин, Александр Валентинович Хоперсков✉

Волгоградский государственный университет,
Волгоград, Россия, khoperskov@volsu.ru✉

Аннотация. Сепарация твердых частиц от газового потока в циклонных устройствах регулируется сложными турбулентными потоками внутри рабочей камеры, поэтому точность моделирования динамики газа является ключевым фактором в прогнозировании эффективности очистки входного потока. В исследовании использован метод крупных вихрей (LES) в рамках ANSYS Fluent. Полученные результаты сравниваются с моделью напряжений Рейнольдса (RSM), которая является наиболее точной и широко используемой анизотропной моделью турбулентности для моделирования циклонов на основе RANS. Для проведения более детального анализа временной структуры возмущений в пристеночной области предложено использовать приращения скорости или вычислять локальное ускорение потока. Такой подход позволяет идентифицировать мелкомасштабную динамику быстрых возмущений, которые обычно скрываются при использовании традиционных методов усреднения по времени. Вычислительные эксперименты с использованием модели LES выявляют наличие мелкомасштабных вытянутых структур, известных как пристеночные полосы. Эти структуры движутся вдоль твердых поверхностей в пристеночной области циклона. Подобные полосатые структуры образуются внутри пограничного слоя. Предложенный метод на основе локальных ускорений позволяет детально исследовать процессы подсеточного масштаба в рамках LES-моделирования. Локальные ускорения, связанные с этими полосатыми возмущениями, могут достигать величины 100 g. Это может негативно повлиять на эффективность разделения и усилить абразивный износ стенок. Приведены оценки фазовой скорости и времени жизни этих нелинейных возмущений вблизи стенки. Эти оценки согласуются с результатами прямого численного моделирования (DNS) для генерации вихревых структур в пограничных слоях. Турбулентная модель RSM, напротив, не позволяет разрешить эти полосатые структуры при анализе локальных полей ускорения.

Ключевые слова: циклонный сепаратор, турбулентный поток газа, вычислительная гидродинамика, метод крупных вихрей

Благодарности: работа выполнена при поддержке Министерства науки и высшего образования Российской Федерации в рамках проекта FZUU-2026-0005. Были использованы вычислительные ресурсы суперкомпьютерного центра Волгоградского государственного университета и лаборатории искусственного интеллекта и анализа данных.

Для цитирования: *Савин Е. С., Хоперсков А. В.* Моделирование потоков газов в циклонном пылеуловителе: динамика мелкомасштабных возмущений в пристеночной зоне // Вестник Астраханского государственного технического университета. Серия: Управление, вычислительная техника и информатика. 2026. № 3. С. 7–18. https://doi.org/10.24143/2072-9502-2026-3-7-18. EDN DCSNLA.

Introduction

The history of using apparatuses with rotating gas for solid particle separation spans more than 100 years [1–3]. It is possible to distinguish axial-flow cyclones [4], apparatuses with tangential gas inlets [5], counterswirling flow cyclones [6, 7], multicyclones [8], and other types. A vast number of diverse designs have been proposed to address specific technological challenges [9–11]. A patent review [12] demonstrates a wide range of technical solutions aimed at reducing the negative impact of atmospheric emissions. Special requirements are imposed on apparatuses used in powder printing [13], the construction industry [14], the agricultural sector [15], mechanical engineering [16], and other industries. The use of separators in the chemical industry is a separate challenge [17, 18]. In this field, they act as integral parts of the technological process, enabling the recovery of catalysts or other valuable components.

Numerical simulation of gas-dynamic processes inside cyclone separators has become the primary research tool, as traditional empirical models do not account for the true complexity of vortex flows [2, 11, 19]. Solid particles follow complex trajectories within a three-dimensional unsteady flow structure, where a peripheral downward vortex transforms into an inner upward vortex. Numerical analysis enables the identification of reverse flow zones, secondary flows, and ‘short-circuiting’ effects, where gas escapes into the vortex finder by bypassing the separation zone. These phenomena are difficult to capture using in-situ sensors inside an operating apparatus in physical experiments.

Optimization of the geometric parameters and operating modes of a cyclone based on numerical experiments allows testing hundreds of configurations without building costly prototypes, including sensor and data processing systems [2, 5, 8, 11, 19]. The pressure drop $\Delta \boldsymbol{p}$ in a cyclone directly determines the power consumption for the separator operation, so simulation is an effective tool for optimizing economic costs, considering the high sensitivity of the $\Delta \boldsymbol{p}$ value to the design. Mitigating abrasive wear under conditions of constant impacts of solid particles against the housing walls at high velocities is considered important. Simulation shows zones of high metal erosion, which allows reinforcing these areas or changing the cyclone geometry [20]. Conducting physical experiments is dangerous and expensive under extreme conditions of high temperatures and pressures, which is typical for the chemical industry. The computational model allows accounting for changes in gas viscosity and density at any temperatures and pressure.

A key factor in cyclone physics is turbulence and the unsteady nature of flows [2, 11, 19]. Their influence on separation efficiency manifests across various spatial and temporal scales. Turbulent velocity fluctuations translate particles chaotically. This produces a negative effect because if a particle is already near the wall, a random turbulent fluctuation can return it back into the central upward flow. In addition to turbulence, a source of strong unsteadiness is the vortex core precession, where the center of the vortex rope oscillates relative to the geometric axis of the apparatus [21]. These low-frequency velocity and pressure changes can lead to a number of consequences. Due to the displacement of the vortex axis, the centrifugal force field loses its axial symmetry. This dynamic factor makes the particle trajectories increasingly chaotic. The vortex core precession near the cyclone bottom creates a vacuum cleaner effect, pulling particles from the dust hopper back into the main flow. Finally, the oscillations of the vortex rope at the top, in the vicinity of the vortex finder inlet, make the boundary between the downward and upward flows unsteady. This creates conditions for the raw gas to break through from the outer zone directly into the vortex finder (the 'short circuit' effect), bypassing the separation zone in the cone. Thus, the physical processes listed above reinforce the instability of particle motion trajectories. This almost always negatively affects separation efficiency, hindering the deposition of fine fractions and promoting their entrainment into the central upward flow.

The aim of this work is to develop a method for processing numerical simulation results of gas dynamics in a cyclone separator to analyze the small-scale flow structure, primarily near the apparatus walls.

Materials and methods

The classic separator is the Stairmand design, consisting of an upper cylindrical section and a lower cone (Fig. 1, *a*).

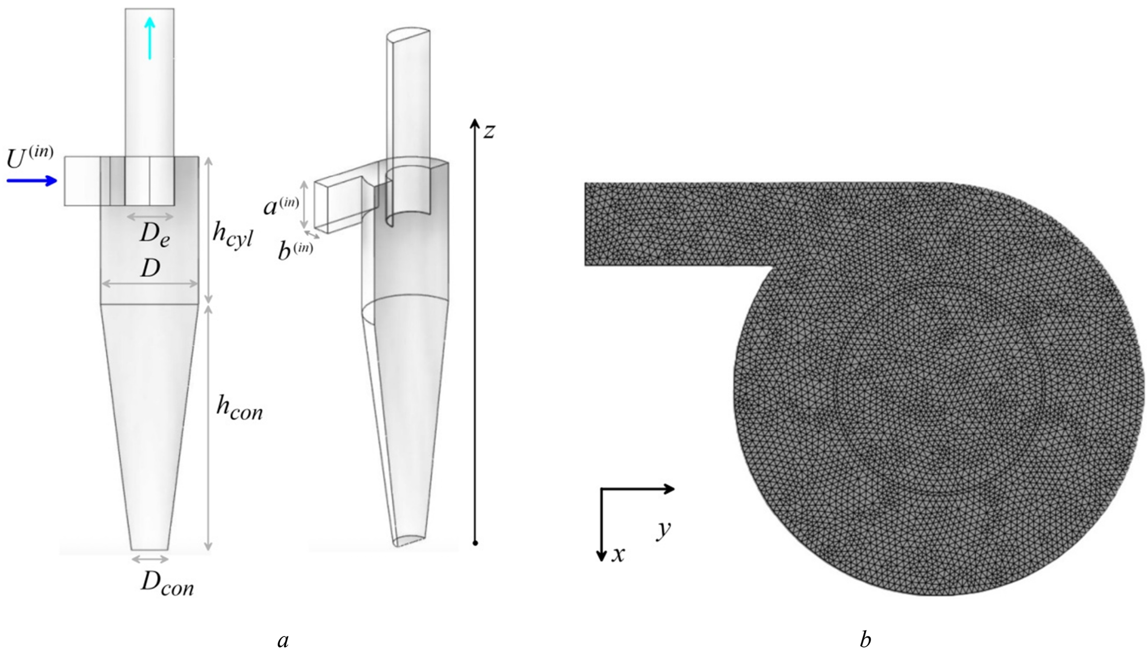

Fig. 1. Geometry of the simulated cyclone (*a*), computational mesh (*b*):
$U^{(in)}$ – inlet velocity direction; D_e – vortex finder diameter; D – cylinder part diameter; D_{con} – cone lower part diameter; h_{cyl} – cylinder section height; h_{con} – cone section height; $a^{(in)}$ – inlet tube height; $b^{(in)}$ – inlet tube width

Gas enters at a velocity of $U^{(in)}$ through a side inlet at the top of the cylinder, creating a highly swirling flow with an azimuthal velocity of $U_\varphi(\boldsymbol{r})$. The rotating gas descends in a spiral in the outer part of the apparatus to the bottom of the cone and rises along the paraxial zone, exiting through the vortex finder at the top. The result is the formation of a global vortex in the cyclone, which consists of a core (vortex rope) in the paraxial region with a linearly growing velocity $U_\varphi \propto r$, and an outer vortex region ($U_\varphi \propto r^{-n_v}$, $n_v > 0$) (the so-called quasifree vortex). The centrifugal force resulting from the rapid rotation of the flow forms the basis of the physical mechanism of gas and solid particle separation.

Constructing the velocity field in a cyclone in accordance with physical measurement data requires considering turbulence. Numerous results indicate the advantages of anisotropic turbulence models. For instance, the Reynolds Stress Model (RSM) and Large Eddy Simulation (LES), including their various modifications, are more appropriate compared to isotropic models ($k-\omega$, $k-\varepsilon$, v^2-f, Menter's SST model, etc.) [11, 13]. The former reproduce the vortex core dimensions and the peripheral rotational velocity decay with $n_v \approx 0.6$ more accurately. We adopt the LES model for this work. Although computationally expensive compared to RSM, it yields direct resolution of unsteady macrostructures. LES computes instantaneous gas velocities at large and medium scales, and only the smallest vortex structures are modeled within the subgrid-scale physics [21]. RSM computes the time-averaged values of the Reynolds stress tensor components and, strictly speaking, does not yield instantaneous fluctuation velocities. This difference is decisive for our study. It should be noted that the majority of contemporary research on cyclone simulation is based on RSM. The application of LES remains limited due to its computational complexity.

At typical operating velocities of $U^{(\text{in})} \lesssim 30$ m/s, the gas inside the cyclone can be considered incompressible with a constant density ϱ. The filtered Navier–Stokes equations used in the LES approach take the following form:

$$\varrho \frac{\partial \bar{U}}{\partial t} + \varrho \nabla \cdot \left(\bar{\boldsymbol{U}} \otimes \bar{\boldsymbol{U}} \right) = -\nabla \bar{p} + \nabla \left[\left(\mu^{(m)} + \mu_{sgs}^{(t)} \right) \left(\nabla \bar{\boldsymbol{U}} + \left(\nabla \bar{\boldsymbol{U}} \right)^T \right) \right] + \varrho \mathbf{g}, \tag{1}$$

where $\bar{\boldsymbol{U}}$ – filtered velocity resolving large-scale eddies; ∇ – nabla operator; $\bar{p}$ – filtered pressure; $\mu^{(m)}$ – molecular dynamic viscosity; $\mu_{sgs}^{(t)}$ – subgrid-scale (SGS) turbulent viscosity; T – operator of transposition; $\boldsymbol{g}$ – gravitational acceleration.

The three spatial components in Cartesian or cylindrical coordinate systems are denoted by the indices $(i, j, k) = (x, y, z)$ or (r, φ, z), respectively. Filtering is performed at the subgrid level and is governed by the dependence of $\mu_{sgs}^{(t)}$ on the grid cell size Δl. The Smagorinsky and Wall-Adapting Local Eddy-viscosity (WALE) models establish a quadratic relationship $\mu_{sgs}^{(t)} \propto (\Delta l)^2$. However, the WALE model incorporates both the strain rate tensor $\hat{S}_{ij}$ and the rotation through the vorticity tensor $\boldsymbol{\Omega}_{ij}$. This automatically ensures the proper near-wall viscosity damping ($\mu_{sgs}^{(t)} \to 0$) and accurately describes the solid-body rotation within the vortex core region, where $U_\varphi \propto r$.

The gas dynamics simulation is performed within a classic high-efficiency cyclone proposed by Norman Stairmand (see Fig. 1, *a*) with the following geometric parameters: $D = 0.29$ m, $D_e = 0.145$ m, $h_{cyl} = 0.435$ m, $h_{con} = 0.725$ m, and $D_{con} = 0.108$ m. For the computations, a 3D model of the apparatus was developed in Autodesk Inventor CAD software and subsequently integrated into Fluent. The calculations are based on triangulated computational meshes (see Fig. 1, *b*). The baseline number of cells in the model is $N^{(g)} = 2.279.176$. The flow-wall interaction is modeled using the Kader blending near-wall treatment. Unlike standard methods, this function provides highaccuracy profile matching in both the viscous sublayer and the logarithmic region of the boundary layer. This is achieved through a nonlinear hybrid approximation that guarantees the continuity of velocity and its derivatives during the transition from the viscous (linear) regime to fully developed turbulent flow.

The subgrid-scale turbulent viscosity is modeled using the WALE approach [22]:

$$\mu_{sgs}^{(t)} = \varrho C_w^2 \left(\Delta l \right)^2 \frac{\left(\bar{S}_{ij}^d \bar{S}_{ij}^d \right)^{\frac{3}{2}}}{\left(\bar{S}_{ij} \bar{S}_{ij} \right)^{\frac{5}{2}} + \left(\bar{S}_{ij}^d \bar{S}_{ij}^d \right)^{\frac{5}{4}}},$$

$$\bar{S}_{ij} = \frac{1}{2} \left(\frac{\partial \bar{U}_i}{\partial x_j} + \frac{\partial \bar{U}_j}{\partial x_i} \right),$$

where C_w – WALE model constant; $\bar{S}_{ij}$ – strain rate tensor defined via the outer product of the nabla operator and the velocity vector calculated from the filtered velocities; $\bar{S}_{ij}^d$ – denotes the traceless symmetric part of the square of the velocity gradient tensor [22].

This definition of $\bar{S}_{ij}^d$ incorporates information about both shear strain and vorticity. A specific combination of these terms in the WALE model allows them to cancel out in solid-body rotation zones, which vanishes in zones of pure solid-body rotation. Repeated indices are summed over. The WALE model constant C_w determines the subgrid-scale dissipation intensity. Its default value is $C_w = 0.325$, providing the best agreement with the exact energy spectrum of decaying isotropic turbulence [22]. Varying this parameter within the 0.2-0.5 range allows for viscosity control. Specifically, selecting $C_w < 0.325$ enables the resolution of smaller eddies but requires a finer mesh to avoid numerical instability. Conversely, choosing $C_w > 0.325$ over-dampens the flow, reducing the inherent advantages of the LES approach. The overbar symbol denoting filtered velocity and pressure variables will be omitted hereafter.

At the cyclone inlet, a velocity of $U^{(in)} = 20$ m/s is specified with a gas density of $\varrho = 1.225$ kg/m^3, which yields a Reynolds number of Re = $3.85 \cdot 10^5$. The inlet flow is characterized by a relative turbulence intensity of I = 0.037 and a hydraulic diameter of 0.082 m. The pipe length is sufficient to develop a velocity profile across the cross-section that is independent of the boundary conditions. The gas outflow from the vortex finder is governed by specifying the "Outflow" boundary condition in Fluent. This corresponds to free boundary conditions utilizing data extrapolation from adjacent grid cells. The average outlet velocity equals $U^{(in)}$ once a quasi-steady-state regime is established.

Parallel computations were performed on workstations equipped with Intel Xeon Gold 6248 (20 cores, 40 threads, 192 GB RAM) and Intel Xeon E5-2698 (20 cores, 40 threads, 512 GB RAM) processors.

Results and discussion

To analyze small-scale rapid fluctuations, it is proposed to consider velocity increments:

$$\delta \boldsymbol{U}^n(\boldsymbol{r}) = \delta \boldsymbol{U}(\boldsymbol{r}, t_n) = \boldsymbol{U}(t_n) - \boldsymbol{U}(t_{n-n_\delta}), \qquad (2)$$

by calculating velocity differences at a given grid node $\boldsymbol{r}$ at two close time instances t_n and t_{n-n_δ}, where $\delta t = t_n - t_{n-n_\delta}$. It should be emphasized that velocity increments characterize temporal velocity changes rather than the fluctuation values themselves.

A quasi-steady-state velocity distribution is established approximately 1 second after the start of the computation, which is due to the small dimensions of the cyclone. Fig. 2 shows the dynamics of tangential velocity increments in the near-wall layer within three cross-sections at different heights z = 0.225, 0.775, 1.075 m.

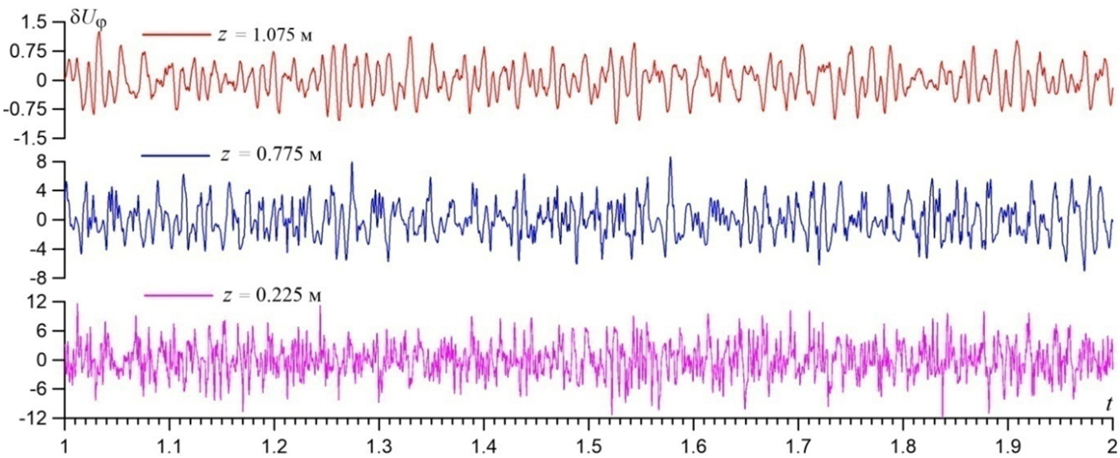

Fig. 2. Computational results for the velocity fluctuation dependence on time in the LES model at three different points of the cyclone

The upper zone above the vortex finder inlet is the calmest. The time dependence $\delta U_\varphi(t)$ at a height of z =1.075 m exhibits a small amplitude within 1.3 m/s with a typical average period of 0.012 s, which yields a frequency of $\omega^{(1)}$ = 520 rad/s. These oscillations reflect large-scale turbulent fluctuations, which is consistent with the estimated time for a single gas revolution, $\omega \sim 2\pi U^{(in)}/D$ = 433 rad/s.

The amplitude of the rotational velocity increment increases to 5-8 m/s below the vortex finder, in the transition zone from the cylindrical part to the conical section at a height of z = 0.775 m (see Fig. 1). Moreover, the nature of the fluctuations changes, with an increase in high-frequency components observed against the background of a typical fluctuation frequency of $\omega^{(2)}$ = 630 rad/s. We attribute this to the enhanced generation of turbulent vortices in the near-wall region and the partial influence of the vortex core precession. In the lower part of the cone at the point z = 0.225 m, the aforementioned processes intensify. The amplitude of the velocity increment can reach 12 m/s, with high-frequency harmonics dominating the behavior of $\delta U_\varphi(t)$. This is due to the unsteady chaotic behavior of the vortex rope end, considering the proximity of the walls at the bottom of the cone.

Dividing the velocity increment by the time interval δt_{n_δ} yields the local acceleration rate:

$$\delta_t \boldsymbol{U} = \frac{\delta \boldsymbol{U}^n_{i,j,k}}{\delta t_{n_\delta}}, \qquad (3)$$

where the choice of the increment $\delta t_{n_\delta} = t_n - t_{n-n_\delta}$ can influence the result and requires additional analysis. Calculation with $\delta t_1 = \Delta t = t_n - t_{n-1}$ (Δt is the time integration step) represents the formally exact definition of the partial time derivative $\partial \boldsymbol{U} / \partial t$. As $\delta t \to 0$, the ratio $\delta \boldsymbol{U} / \delta t$ approximates the instantaneous local acceleration of the flow. However, under developed turbulence and two-phase flow conditions, instantaneous grid estimates at a single integration step are prone to strong random fluctuations (numerical noise). To eliminate these oscillations and extract large-scale dynamic trends, a numerical smoothing procedure over the time interval $n_\delta = 5$ is applied when calculating $\delta_t U$. It is necessary to emphasize the physical meaning of equation (3). It characterizes the non-stationarity of the velocity field at a fixed grid point, which strictly corresponds to the Eulerian description of a continuous medium. Consequently, this local acceleration omits the convective transport term $\nabla\bullet(U \otimes U)$ from equation (1). Transition to the Lagrangian description requires the total (substantial) derivative: $dU / dt = \partial U / \partial t + (U \bullet \nabla)U$. This total derivative determines the true acceleration of an individual fluid volume or a solid dust particle by combining local non-stationarity with convective transport.

Utilizing the velocity increment (2) or the local acceleration operator δt (3) offers several advantages over analyzing absolute velocity values. First, the mean tangential velocity $\langle \boldsymbol{U}_\varphi \rangle$ in a cyclone is high and can double the inlet velocity $\boldsymbol{U}^{(in)}$. Against the background of such an intense primary flow, small-scale and high-frequency pulsations are difficult to quantify or visualize. The velocity increment automatically filters out the stationary or slowly varying flow components. This filtration isolates the non-stationary dynamics and transient perturbations. Consequently, $\delta \boldsymbol{U}(t)$ and $\delta_t \boldsymbol{U}(t)$ highlight the fastest physical processes. These rapid processes play a critical role in degrading the particle separation efficiency. Second, the proposed approach enables the identification of coherent structures and the visualization of perturbation fronts, including the vortex core region. Third, the $\delta \boldsymbol{U}$ values allow for analyzing energy transfer across the turbulence spectrum during the energy cascade process.

Constructing the spatial distributions of $\delta \boldsymbol{U}(\boldsymbol{r}, t)$ and $\delta_t \boldsymbol{U}(\boldsymbol{r}, t)$ requires interpolating data from an unstructured mesh (see Fig. 1) onto a regular grid in various cross-sectional planes. Let us first consider the numerical results obtained using the RSM, which provides the components of the Reynolds stress tensor $\widehat{R}_{ij} = \overline{u_i' u_j'}$ for velocity fluctuations. The term $\sqrt{\widehat{R}_{\varphi\varphi}}$ determines the root-mean-square value of the turbulent fluctuations of the gas tangential velocity component. Fig. 3 illustrates the spatial distributions of the local acceleration of the fluctuating component $\delta_t \sqrt{\widehat{R}_{\varphi\varphi}}$ in a vertical plane.

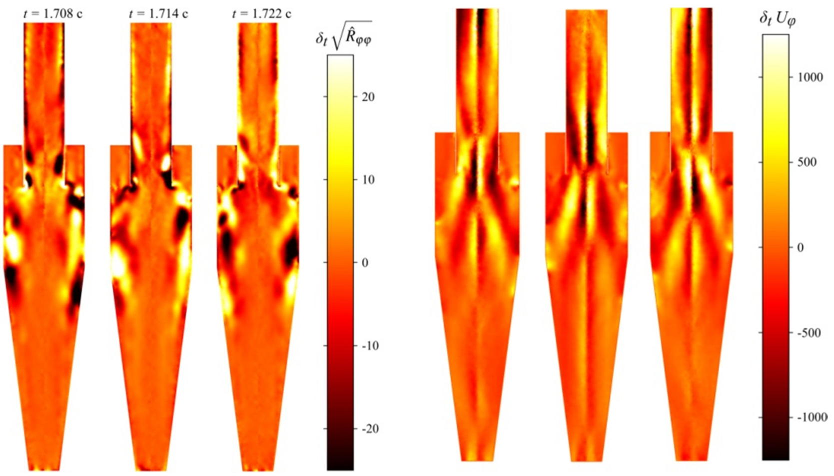

Fig. 3. Representative spatial distributions of the local acceleration based on based on the tangential velocity component $\delta_t \boldsymbol{U}_\varphi$ and the fluctuating component $\delta_t \sqrt{\widehat{R}_{\varphi\varphi}}$ in the $(x, y = 0, z)$ plane, calculated using the RSM turbulence model

Additionally, the $\delta_t U_\varphi$ values were calculated for the mean velocity fields obtained from the RANS equations closed via the RSM approach. These distributions are representative and reveal intense non-stationary perturbations in the lower region of the vortex finder (exhaust pipe). Perturbations are also pronounced within the vortex core region along the cyclone axis and in the exiting gas stream due to the decay of swirl inside the exhaust pipe. The primary conclusion regarding vortex generation in the boundary layer is the inherent inability of the RSM approach to resolve these structures. This limitation arises because the local accelerations $\delta_t \sqrt{\widehat{R}_{\varphi\varphi}}$ are nearly two orders of magnitude smaller than $\delta_t \boldsymbol{U}_\varphi$. In this modeling framework, turbulence generation occurs strictly at the subgrid level via source terms. Consequently, macro-flow analysis fails to detect discrete near-wall vortex structures where the $\delta_t \sqrt{\widehat{R}_{\varphi\varphi}}$ values remain negligibly small.

Fig. 4 displays the spatial distributions of the local accelerations $\delta_t \boldsymbol{U}_\varphi$ obtained via LES.

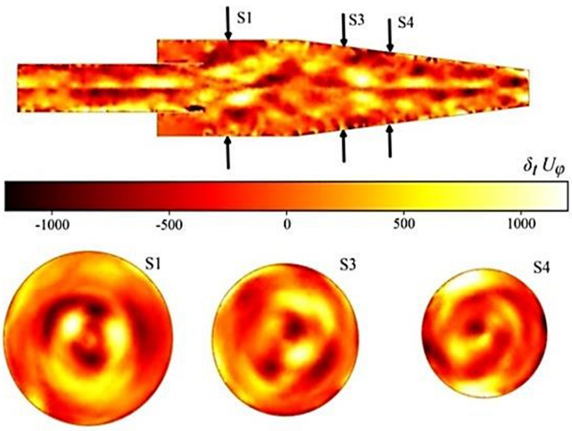

Fig. 4. Representative spatial distributions of the local tangential gas acceleration calculated using the LES model in the longitudinal (x, $y = 0$, z) planes and across three transverse planes S1, S2, and S3

This approach clearly identifies the high-frequency non-stationary structures within the flow. Of particular interest are the near-wall formations. In the meridian plane, they appear as alternating chains of extrema along the apparatus walls. In the transverse cross-sections, these perturbations exhibit a characteristically thin, elongated shape. This topology aligns with modern concepts of near-wall turbulence generation mechanisms. Specifically, direct numerical simulations (DNS) demonstrate the elongation of vortex tubes and the formation of coherent streak structures oriented along the primary flow direction [23]. Crucially, the proposed analysis method does not merely capture static spatial inhomogeneities in the velocity field. Instead, it serves as a dynamic map reflecting the temporal evolution of these vortex structures.

For each time instant, the spatial distributions of the variables (2) and (3) are determined, from which the coordinates of the local spatial extrema are isolated. Specifically, these include the minima for negative perturbations and the maxima for positive perturbations of the local flow acceleration (Fig. 5).

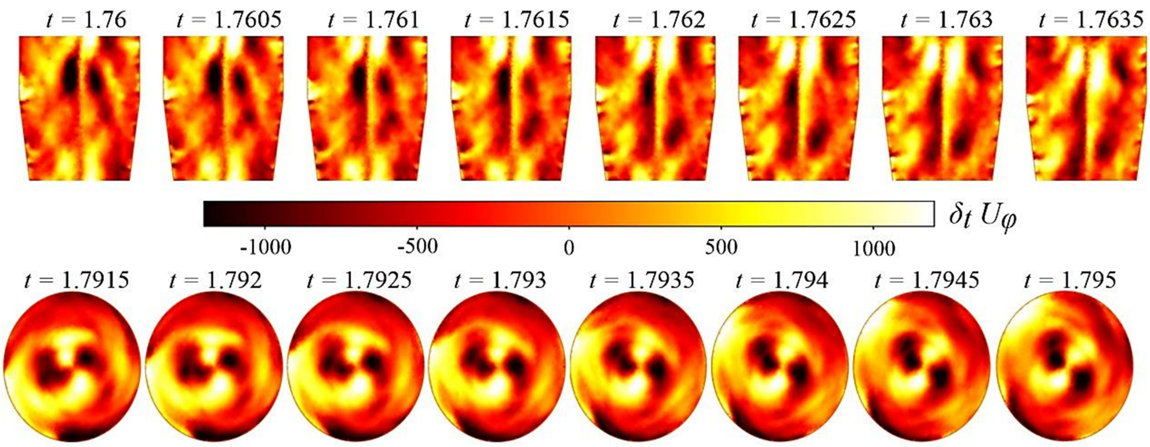

Fig. 5. Temporal evolution of the local tangential gas acceleration fields calculated via LES at consecutive time steps

Calculating the vertical displacement δz_{n_δ} of the extremum point over a small time interval δt_{n_δ} yields the phase velocity of the perturbation:

$$V^{(\delta)}_{ph,z} = \frac{\delta z_{n_\delta}}{\delta t_{n_\delta}}. \tag{4}$$

The phase velocity estimation (4) is performed within a fixed vertical (meridional) cross-section of the cyclone.

The lifetime of streak structures $\tau_{streak} \simeq t^+ \nu^{(m)} / u^2_{\tau 0}$ depends primarily on the kinematic molecular viscosity $\nu^{(m)} = \mu^{(m)} / \rho$ and the wall shear velocity $u_{\tau 0}$. This shear velocity is expressed directly via the wall shear stress. Direct numerical simulations (DNS) of near wall vortex generation estimate the dimensionless time as $t^+ \simeq$ 100-400 before the vortex detaches from the wall. This value can exceed $t^+ \simeq 700$ during the vortex dissipation stage [23]. Assuming $u_{\tau 0} \simeq$ 0.5-1.0 m/s, the estimated lifetime falls within the range of 0.002-0.02 s. Fig. 6 presents the calculated phase velocities along the z coordinate for a sample of streak structures obtained via LES.

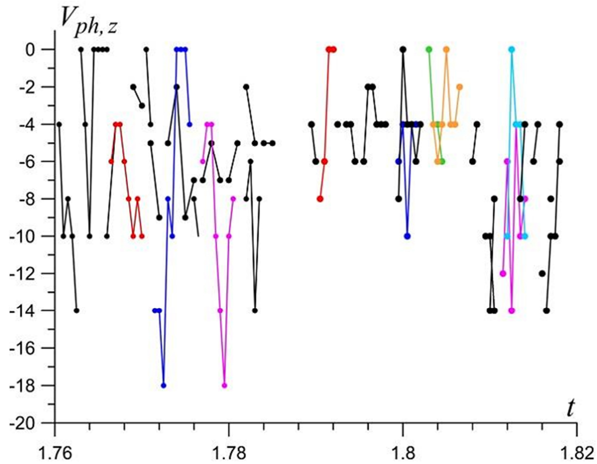

Fig. 6. Spatial distribution of the vertical phase velocity component belonging to small scale near wall gas perturbations

Each line tracks a single structure from its inception to disappearance. The lifetime observed in Fig. 6 is generally shorter than the DNS estimate.

This discrepancy stems from the specific perturbation tracking method applied in this work. Due to the high swirl velocity, the streak structure satisfies the condition $V^{(\delta)}_{ph,\varphi} \gg V^{(\delta)}_{ph,z}$. Consequently, the structure often exits the analyzed meridional plane before its actual destruction. The representative vertical phase velocities in Fig. 6 vary between 0 and 19 m/s. The proposed extremum isolation technique combined with a small gas dynamics integration step of Δt = 0.0001 s yields a phase velocity error of approximately 1 m/s. This relative error of 5% reliably distinguishes slow structures from fast ones. It ensures the capture of true physical evolution rather than numerical noise. For a sample of streak structures over a time interval of 0.05 seconds, Fig. 7 presents the phase velocity distribution $\phi(V^{(\delta)}_{ph,z})$.

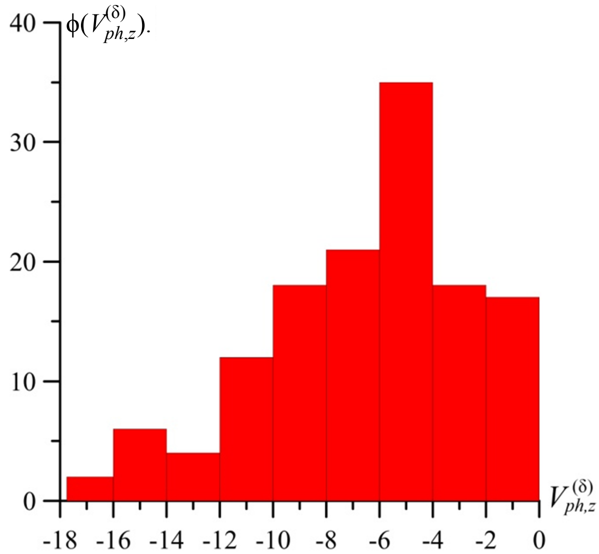

Fig. 7. Distribution of the vertical phase velocities of coherent streak structures within the numerical mode

The distribution exhibits a pronounced peak in the phase velocity range from 4 to 6 m/s. This interval closely matches the near wall axial gas velocity which varies from 4 to 9 m/s. Consequently, a significant portion of the structures undergoes transport by the primary flow due to advection. The established range of streak structure phase velocities from 0 to 19 m/s demonstrates high dynamic heterogeneity within the near wall layer. The achieved accuracy of 1 m/s in determining the perturbation phase velocity is sufficient for an accurate description of the interaction between fine particles and coherent flow structures. This sufficiency arises because the characteristic scale of velocity variation within the structures substantially exceeds the numerical error level. The vertical phase velocity component of certain streak structures can significantly exceed the mean local values of the vertical gas velocity. This phenomenon indicates that the vertical dynamics of perturbations in the near wall zone of the cyclone depend not only on drift by the primary flow but also on intense interaction with the high velocity rotating core. The elevated phase velocity of individual structures indicates the existence of mechanisms for rapid momentum transport along the conical walls of the apparatus. This conclusion is critically important for understanding and predicting the trajectories of fine particles.

The LES method explicitly resolves vortex structures with a minimum spatial scale of three to five cell sizes. Scales below two cell sizes are parameterized within the subgrid scale physics. Consequently, the question regarding the actual geometric dimensions of the detected near wall perturbations requires further investigation. This investigation necessitates calculations on substantially finer grids capable of resolving the boundary layer. The thickness of the viscous laminar sublayer in the analyzed cyclone ranges from 0.08 to 0.09 mm. Furthermore, a transition zone is located between approximately 0.09 and 0.5 mm from the wall where turbulent vortices begin to generate. Above 0.5 mm and up to 30 mm lies a fully turbulent logarithmic layer whose dynamics are governed by the solid boundary effect. Considering the relationship between the cell size and the total cell count, high quality resolution of vortex structures within the boundary layer requires a near wall grid spacing of 0.1 mm. Even with local mesh refinement techniques, this requirement demands approximately two hundred million cells. Such a computational scale shifts these models toward DNS. The application of DNS methods for modeling cyclone separators at high Reynolds numbers is limited by extreme computational complexity. This limitation stems from the power law dependence of the total cell number and the integration time step on the Reynolds number. Therefore, the proposed analysis of velocity increments and local accelerations is of significant interest. It provides an opportunity to evaluate the properties of coherent streak structures and vortex generation mechanisms within the cyclone boundary layer using LES models with a relatively moderate cell count.

Conclusion

To perform a comprehensive analysis of spatial perturbations within the cyclone separator chamber, a method based on evaluating gas velocity increments $\delta \boldsymbol{U}$ and local accelerations $\delta_t \boldsymbol{U}$ via LES modeling was developed and proposed according to equations (2) and (3). This approach identifies coherent near wall streak structures despite the subgrid mechanism of their generation in numerical cyclone models using moderate computational meshes of only a few million cells. The calculated phase velocities and lifetimes of these coherent structures demonstrate satisfactory agreement with fundamental data from direct numerical simulations DNS. The proposed method is also highly effective for investigating the non stationary dynamics of the precessing vortex core. It is established that the local gas accelerations can reach extreme values of up to 100 g and above within both the axial zone of the vortex core and the near wall region of the cyclone. The achieved accuracy of 1 m/s in determining the phase velocity is sufficient for an accurate description of the interaction between fine particles and coherent flow structures.

High frequency near wall gas pulsations induce the detachment of the solid phase from its calculated trajectories. Due to their specific inertia, dust particles adapt to smooth and slow variations of the carrier flow, thereby maintaining their motion along the apparatus wall. Conversely, rapid pulsations exert an impulsive dynamic impact on the dispersed phase. When the characteristic duration of a pulsation is comparable to the dynamic relaxation time of a solid particle, the particle is instantaneously ejected from the boundary layer back into the central upward flow. This phenomenon represents the primary mechanism of secondary dust re-entrainment. This mixing induces continuous suspension of the dispersed layer near the conical walls of the apparatus. Consequently, it prevents the deposition of fine particle fractions into the dust hopper, thereby reducing the overall separation efficiency.

Precession of the vortex core contributes significantly to the non stationary behavior of $\delta \boldsymbol{U}$ and $\delta_t \boldsymbol{U}$. High frequency pulsations induce chaotic bending and spatial oscillation of the vortex rope. Under a stable vortex rope configuration, the separation process follows the classical mechanism where the dispersed phase undergoes centrifugal transport toward the walls followed by slow deposition. Conversely, rapid spatial displacements of the vortex axis alter the local pressure field. Consequently, the low pressure zone developing at the center intensely entrains fine particles from the flow periphery. This phenomenon causes a sharp degradation in fractional separation efficiency, particularly for fine dust fractions. Finally, the short circuiting of contaminated gas beneath the vortex finder is also functionally related to rapid velocity and pressure pulsations generated directly below the exhaust pipe cut. These perturbations induce the formation of short lived gas transport channels. Through these non stationary channels, solid particles bypass the primary separation zone of the apparatus and penetrate directly into the vortex finder.

Turbulence models belonging to the RSM family fundamentally fail to describe the true non stationary dynamics of near wall vortex structures. The observed fifty fold excess of the mean velocity increments $\delta_t \boldsymbol{U}$ over the increments of turbulence characteristics calculated via the Reynolds stress tensor is explained by the dominance of macroscopic non stationarity induced by the vortex core precession. Within the RSM framework, the mean velocity field dynamically adjusts to the spatial displacement of the vortex axis in zones of high spatial gradients. Conversely, the turbulent stress field exhibits high inertia and a more smoothed spatial distribution. It is established that the RSM approach systematically underestimates the dynamics of turbulent characteristics, demonstrating stress increments nearly two orders of magnitude smaller than those of the mean velocity. This phenomenon proves the inapplicability of the RANS family approaches for analyzing rapid local processes inside cyclone separators. Consequently, it mathematically justifies the necessity of utilizing LES models for accurate prediction of the instantaneous dynamic impacts exerted by the carrier flow on the dispersed phase.

References

1. Fadin Yu. M., Bogdanov V. S., Yur'eva M. V., Vechkanov A. V. Vozvratno-potochnye ciklony. Istoki vozniknoveniya i napravleniya sovershenstvovaniya [Reciprocating cyclones. The origins and directions of improvement]. *Vestnik BGTU imeni V. G. Shuhova*, 2017, no. 5, pp. 104-109.

2. Ayl E., Kocak E. A comprehensive review of cyclone separator technology. *The Canadian Journal of Chemical Engineering*, 2024, vol. 103, no. 6, pp. 2751-2789.

3. Rivera-Garcia M. O., Reyna M. A., Camarillo-Ramos M. A., Reyna-Vargas M. A., Avitia R. L., Cuevas Gonzalez D., Osornio Vargas A. R. Cyclone Separator for Air Particulate Matter Personal Monitoring: A Patent Review. *Atmosphere*, 2023, vol. 14, no. 4, id. 624.

4. Toptalov V. S., Chesnokov Yu. G., Meshalkin V. P., Kulov N. N., Flisyuk O. M., Marculevich N. A., Lihachev I. G. Ocenka effektivnosti razdeleniya pylegazovyh potokov v pryamotochnyh ciklonah [Evaluation of the efficiency of separa-tion of dust and gas flows in direct-flow cyclones]. *Teoreticheskie osnovy himicheskoj tekhnologii*, 2023, vol. 57, no. 4, pp. 363-370.

5. Vivek R., Venkatesh S., Manoj V., Kumar M., Mohanasundaram. A brief review on improving materials particulates using cyclone separator by geometrical and turbulence factors. *Materials Today: Proceedings*, 2022, vol. 69, no. 3, pp. 1076-1079.

6. Azarov V. N., Azarov D. V. *Pyleuloviteli so vstrechnymi zakruchennymi potokami* [Dust collectors with counter swirling streams]. Volgograd, Izd-vo VolgGTU, 2020. 140 p.

7. Sakharova A. A., Sorokin A. Yu., Azarov D. V., Lupinogin V. V. The effectiveness of the dust particles of the flask in the apparatus of counter-swirling flows. *IOP Conference Series: Materials Science and Engineering*, 2021, vol. 1083, id. 012099.

8. He W., Yang J., Sun G. Inserting an Additional Vortex Finder to Improve the Performance of Cyclones in Series. *Separations*, 2025, vol. 12, no. 1, id. 60.

9. Gol'cov A. B., Logachev K. I., Tiron O. V. *Vihrevaya ventilyaciya. Zakruchennye recirkulyacionnye, otryvnye pylevozdushnye techeniya* [Vortex ventilation. Swirling recirculating, detachable dust-air currents]. Belgorod, Izd-vo BGTU, 2025. 349 p.

10. Katin V. D., Ahtyamov M. H., Dolgov R. V. *Modernizaciya i razrabotka novyh effektivnyh zolo- i pyleulovitelej dlya zashchity sredy obitaniya cheloveka* [Modernization and development of new effective ash and dust collectors to protect the human environment]. Moscow, Sputnik+ Publ., 2015. 116 p.

11. Savin E. S., Hoperskov A. V. Obzor chislennyh modelej pyleulovitelej ciklonnogo tipa [Overview of numerical models of cyclone type dust collectors]. *Matematicheskaya fizika i komp'yuternoe modelirovanie*, 2025, vol. 28, no. 4, pp. 54-106.

12. Vasil'ev A. V. Obzor patentov i tekhnicheskih reshenij po snizheniyu negativnogo vozdejstviya vybrosov v vozdushnuyu sredu v usloviyah urbanizirovannyh territorij [Review of patents and technical solutions to reduce the negative impact of air emissions in urbanized areas]. *Izvestiya Samarskogo nauchnogo centra Rossijskoj akademii nauk*, 2025, vol. 27, no. 3-2, pp. 440-451.

13. Polieftova A. P., Sedlyarov O. I., Otrubyannikov E. V. Chislennoe issledovanie effektivnosti ciklonov, primenyaemyh v apparatah poslojnogo sinteza metodom selektivnogo lazernogo splavleniya [Numerical investigation of the effectiveness of cyclones used in layer-by-layer synthesis devices by selective laser fusion]. *Promyshlennye processy i tekhnologii*, 2025, vol. 5, no. 3, pp. 82-91.

14. Krasovickij Yu. V., Nikolaev V. I., Piglovskij N. V., Fedorova M. N. Konstrukcii, raschet i aerodinamicheskaya optimizaciya vihrevyh pyleulovitelej v proizvodstve stroitel'nyh materialov [Designs, calculation and aerodynamic optimization of vortex dust collectors in the production of building materials]. *Stroitel'nye materialy*, 2010, no. 5, pp. 84-87.

15. Zlochevskij V. L., Muhopad K. A. Aerodinamicheskoe soprotivlenie vintovogo kanala v ciklone separatore [Aerodynamic drag of the screw channel in the cyclone separator]. *Tekhnika i tekhnologiya pishchevyh proizvodstv*, 2017, vol. 46, no. 3, pp. 102-107.

16. Meskhi B. Ch., Gumenyuk A. S., Dzhedirov D. A., Bedoidze M. V. Modeling Dust Disperse Composition when Designing Aspiration Systems of Milling Machines. *Occupational Safety in Industry*, 2025, no. 10, pp. 87-93.

17. Shartdinov A. Sh., Kvyatkovskaya A. S., Epimahov N. L., Silant'eva L. Ya. Primenenie sintez-gaza dlya proizvodstva al'ternativnyh istochnikov energii [The use of synthesis gas for the production of alternative energy sources]. *Sovremennye naukoemkie tekhnologii*, 2021, no. 3, pp. 106-111.

18. Petrov D. N., Chistyakova T. B. Sistema avtomatizirovannogo proektirovaniya i prototipirovaniya uchastkov sinteza uglerodnyh nanoklasternyh struktur [Computer-aided design and prototyping system for the synthesis of carbon nanocluster structures]. *Vestnik Astrahanskogo gosudarstvennogo tekhnicheskogo universiteta. Seriya: Upravlenie, vychislitel'naya tekhnika i informatika*, 2021, no. 3, pp. 16-27.

19. Chen J., Chen Y., Zhang L., Zhao B., Li Y. Numerical Simulation of a Novel Secondary Separation Cyclone. *Processes*, 2025, vol. 13, no. 6, id. 1874.

20. Guo M., Xia G., Guo P., Manickam S., Yoon J. Y., Sun X. Insights into local wall erosion characteristics and

prevention measures for cyclone separators. *International Journal of Fluid Engineering*, 2024, vol. 1, no. 4, id. 040601.

21. Savin E. S., Khoperskov A. V. Comparative Analysis of Turbulent Models for Gas Flow Dynamics in Cyclone Separators. *Technologies*, 2026, vol. 14, no. 5, id.282.

22. Nicoud F., Ducros F. Subgrid-Scale Stress Modelling Based on the Square of the Velocity Gradient Tensor. *Flow, Turbulence and Combustion,* 1999, vol. 62, pp. 183-200.

23. Lozano-Duran A., Jimenez J. Time-resolved evolution of coherent structures in turbulent channels: characterization of eddies and cascades. *Journal of Fluid Mechanics*, 2014, vol. 759, pp. 432-471.

Список источников

1. Фадин Ю. М., Богданов В. С., Юрьева М. В., Вечканов А. В. Возвратно-поточные циклоны. Истоки возникновения и направления совершенствования // Вестн. БГТУ им. В. Г. Шухова. 2017. № 5. С. 104–109.

2. Ayl E., Kocak E. A comprehensive review of cyclone separator technology // The Canadian Journal of Chemical Engineering. 2024. V. 103. N. 6. P. 2751–2789.

3. Rivera-Garcia M. O., Reyna M. A., Camarillo-Ramos M. A., Reyna-Vargas M. A., Avitia R. L., Cuevas Gonzalez D., Osornio Vargas A. R. Cyclone Separator for Air Particulate Matter Personal Monitoring: A Patent Review // Atmosphere. 2023. V. 14. N. 4. Id. 624.

4. Топталов В. С., Чесноков Ю. Г., Мешалкин В. П., Кулов Н. Н., Флисюк О. М., Марцулевич Н. А., Лихачев И. Г. Оценка эффективности разделения пылегазовых потоков в прямоточных циклонах // Теоретические основы химической технологии. 2023. Т. 57. № 4. С. 363–370.

5. Vivek R., Venkatesh S., Manoj V., Kumar M., Mohanasundaram. A brief review on improving materials particulates using cyclone separator by geometrical and turbulence factors // Materials Today: Proceedings. 2022. V. 69. N. 3. P. 1076–1079.

6. Азаров В. Н., Азаров Д. В. Пылеуловители со встречными закрученными потоками. Волгоград: Изд-во ВолгГТУ, 2020. 140 с.

7. Sakharova A. A., Sorokin A. Yu., Azarov D. V., Lupinogin V. V. The effectiveness of the dust particles of the flask in the apparatus of counter-swirling flows // IOP Conference Series: Materials Science and Engineering. 2021. V. 1083. Id. 012099.

8. He W., Yang J., Sun G. Inserting an Additional Vortex Finder to Improve the Performance of Cyclones in Series // Separations. 2025. V. 12. N. 1. Id. 60.

9. Гольцов А. Б., Логачев К. И., Тирон О. В. Вихревая вентиляция. Закрученные рециркуляционные, отрывные пылевоздушные течения. Белгород: Изд-во БГТУ, 2025. 349 с.

10. Катин В. Д., Ахтямов М. Х., Долгов Р. В. Модернизация и разработка новых эффективных золо- и пылеуловителей для защиты среды обитания человека. М.: Спутник+, 2015. 116 с.

11. Савин Е. С., Хоперсков А. В. Обзор численных моделей пылеуловителей циклонного типа // Математическая физика и компьютерное моделирование. 2025. Т. 28. № 4. С. 54–106.

12. Васильев А. В. Обзор патентов и технических решений по снижению негативного воздействия выбросов в воздушную среду в условиях урбанизированных территорий // Изв. Самар. науч. центра Рос. акад. наук. 2025. Т. 27. № 3-2. С. 440–451.

13. Полиефтова А. П., Седляров О. И., Отрубянников Е. В. Численное исследование эффективности циклонов, применяемых в аппаратах послойного синтеза методом селективного лазерного сплавления // Промышленные процессы и технологии. 2025. Т. 5. № 3. С. 82–91.

14. Красовицкий Ю. В., Николаев В. И., Пигловский Н. В., Федорова М. Н. Конструкции, расчет и аэродинамическая оптимизация вихревых пылеуловителей в производстве строительных материалов // Строительные материалы. 2010. № 5. С. 84–87.

15. Злочевский В. Л., Мухопад К. А. Аэродинамическое сопротивление винтового канала в циклоне сепараторе // Техника и технология пищевых производств. 2017. Т. 46. № 3. С. 102–107.

16. Meskhi B. Ch., Gumenyuk A. S., Dzhedirov D. A., Bedoidze M. V. Modeling Dust Disperse Composition when Designing Aspiration Systems of Milling Machines // Occupational Safety in Industry. 2025. N. 10. P. 87–93.

17. Шартдинов А. Ш., Квятковская А. С., Эпимахов Н. Л., Силантьева Л. Я. Применение синтез-газа для производства альтернативных источников энергии // Современные наукоемкие технологии. 2021. № 3. С. 106–111.

18. Петров Д. Н., Чистякова Т. Б. Система автоматизированного проектирования и прототипирования участков синтеза углеродных нанокластерных структур // Вестн. Астрахан. гос. техн. ун-та. Сер.: Управление, вычислительная техника и информатика. 2021. № 3. С. 16–27.

19. Chen J., Chen Y., Zhang L., Zhao B., Li Y. Numerical Simulation of a Novel Secondary Separation Cyclone // Processes. 2025. V. 13. N. 6. Id. 1874.

20. Guo M., Xia G., Guo P., Manickam S., Yoon J. Y., Sun X. Insights into local wall erosion characteristics and prevention measures for cyclone separators // International Journal of Fluid Engineering. 2024. V. 1. N. 4. Id. 040601.

21. Savin E. S., Khoperskov A. V. Comparative Analysis of Turbulent Models for Gas Flow Dynamics in Cyclone Separators // Technologies. 2026. V. 14. N. 5. Id.282.

22. Nicoud F., Ducros F. Subgrid-Scale Stress Modelling Based on the Square of the Velocity Gradient Tensor // Flow, Turbulence and Combustion. 1999. V. 62. P. 183–200.

23. Lozano-Duran A., Jimenez J. Time-resolved evolution of coherent structures in turbulent channels: characterization of eddies and cascades // Journal of Fluid Mechanics. 2014. V. 759. P. 432–471.

The article was submitted 18.03.2026; approved after reviewing 08.05.2026; accepted for publication 25.06.2026
Статья поступила в редакцию 18.03.2026; одобрена после рецензирования 08.05.2026; принята к публикации 25.06.2026

Information about the authors / Информация об авторах

Egor S. Savin – Postgraduate Student of the Department of Information Systems and Computer Simulation; Volgograd State University; e.s.savin@volsu.ru

Alexander V. Khoperskov – Doctor of Physico-Mathematical Sciences, Professor; Head of the Department of Information Systems and Computer Simulation; Volgograd State University; khoperskov@volsu.ru

Егор Сергеевич Савин – аспирант кафедры информационных систем и компьютерного моделирования; Волгоградский государственный университет; e.s.savin@volsu.ru

Александр Валентинович Хоперсков – доктор физико-математических наук, профессор; заведующий кафедрой информационных систем и компьютерного моделирования; Волгоградский государственный университет; khoperskov@volsu.ru